A Generalized Two Point Ellipsoidal Anisotropic Ray Tracing for Converted Waves *

Debora Cores † **Milagros C. Loreto** ‡

May 2005

Abstract

Rocks can be anisotropic due to a variety of reasons. When estimating rock velocities from seismic data, failure to introduce anisotropy into earth models could generate distortions in the final images that can have enormous economic impact. To estimate anisotropic earth velocities by tomographic methods, it is necessary to trace rays or to solve the wave equation in models where anisotropy has been properly considered. Thus, in this work we present a 3-D generalized ellipsoidal travel time formulation that allow us to trace rays in an anisotropic medium. We propose to trace rays in anisotropic media by solving a set of nonlinear optimization problems, where the group velocities for P and S wave propagation modes are 3-D ellipsoidal approximations that have been recently obtained. Moreover, we prove that this 3-D ellipsoidal anisotropic ray tracing formulation is a convex nonlinear optimization problem, and therefore any solution of the problem is a global minimum. Each optimization problem is solved by the global spectral gradient method, which requires first order information and has low computation and low storage requirements. Our approach for tracing rays in anisotropic media is a generalization in the sense that handles titled axis of symmetry and, close to the axis of symmetry, it is an accurate formulation for 2-D transversely isotropic media and 3-D orthorhombic media, depending on the input parameters. Moreover, this formulation gives the exact ray trajectories in 2-D and 3-D homogeneous isotropic media. The simplicity of the formulation and the low computational cost of the optimization method allow us to

*Partially supported by Fonacit project UCV-97-003769

†Departamento de Cómputo Científico y Estadística, and Centro de Estadística y Software Matemático (CESMa), Universidad Simón Bolívar, Apartado 89000, Caracas 1080-A, Venezuela. (E-mail:cores@cesma.usb.ve, fax # 58 212-9063362)

‡Departamento de Computación, Centro de Cálculo Científico y Tecnológico (CCCT), Facultad de Ciencias, Universidad Central de Venezuela, Apartado 47002, Caracas 1041-A, Venezuela. (E-mail: mloreto@kuaimare.ciens.ucv.ve, fax # 58-212-6051131)

present a variety of numerical results that illustrate the behavior and computational advantages of the approach, and the difficulties when working in anisotropic media.

Keywords
Ray tracing, unconstrained optimization, forward modeling, anisotropic media.

1 Introduction

To estimate anisotropic earth velocities by tomographic methods, it is necessary to trace rays or to solve the wave equation in models where anisotropy has been properly considered. Introducing anisotropy in a numerical approach is a complex problem, since analytic or approximated expressions for the group velocity are very complex or difficult to obtain. Besides, the complexity of finding expressions for the group velocity increases when a low symmetry anisotropy is considered, which is the case in an orthorhombic medium.

Today, even with recent computer technology estimating velocities by seismic tomography in anisotropic media requires considerable CPU time, since the tomographic method is an iterative scheme that requires, at each iteration, the travel time function for each pair of sources and receivers in the model, and its ray trajectory. Moreover, the equation for travel time in an anisotropic medium is a highly nonlinear function. For that reason, a low cost and storage technique for tracing rays in 3-D anisotropic media is very crucial.

The problem of tracing rays in isotropic media has been formulated and solved by many authors in the literature, however in anisotropic media, there exist less references in these topics. In particular, Byun (1982) proposed a technique based on Snell's law and on the equations that relate phase and group velocities at each interface, to obtain the rays in inhomogeneous anisotropic media. Pratt and Chapman (1992) and Chapman and Pratt (1992) present a scheme that traces rays in isotropic media and then project them in anisotropic media. Michelena *et al.* (1993) and Michelena (1993) present a 2-D elliptical approximation of the phase velocity and trace rays in 2-D heterogeneous transversely isotropic media. More recently, Grechka and McMechan (1996) present an optimization technique for tracing rays in transversely isotropic media which consider the Thomsen (1986) weak anisotropic parameters.

In this work, we present the problem of tracing rays in an anisotropic medium as a set of optimization problems. Each optimization problem is based on Fermat's principle and the group velocity is approximated by a 3-D ellipsoidal expression, which has been recently obtained by Contreras *et al.* (1997). This expression depends on the values of the NMO velocities on the symmetry planes and the polar and

azimuthal group angles, which simplifies the computations of the objective travel time function and its derivative. This ellipsoidal function is an accurate approximation to the group velocity in 2-D transversely isotropic media and in 3-D orthorhombic media for small phase angle (close to the symmetry axis) with no restrictions on the azimuthal angle. Moreover, this approximation for P and S wave propagation modes generalizes the results obtained by Levin (1978), Byun (1982) and Muir (1990) for transversely isotropic media. Contreras *et al.* (1997) numerically compare the exact and the ellipsoidal impulse responses in orthorhombic media and, they show that this velocity approximation is accurate up to 30^o degrees for P-waves, and up to 40^o degrees for S-waves. It is important to stress that as any other approximation in anisotropic media, for example, Thomsen (1986), Grechka and McMechan (1996), Tsvankin (1996), has a limitation in the range of its application. We also propose to solve each optimization problem with the Global Spectral Gradient (GSG) Method, developed by Raydan (1997). This is a low cost and low storage technique since only gradient evaluations and few floating point operations are required. It is a global scheme, in the sense that convergence is attained from any initial ray path, and it also has fast local convergence. The GSG method has been used recently in some geophysical applications, obtaining computational advantages and good precision, as for example: 3D isotropic heterogeneous ray tracing, Cores *et al.* (2000); tomographic velocity estimation and pre-stack depth migration, Castillo *et al.* (2000), D'Agosto and Michelena (1997) and D'Agosto *et al.* (1998).

The proposed 3-D ellipsoidal anisotropic ray tracing is a general procedure because it is valid near the axis of symmetry regardless of its inclination. Moreover, this ellipsoidal anisotropic expression is a generalized equation, since it can be applied to a transversely isotropic medium and to an orthorhombic medium, depending on the model parameters. So, the travel time formulation developed in this work is a fast and accurate tool to model the travel time close to the axis of symmetry in an orthorhombic media, and to obtain P-P and P-S reflection times in media with tilted axis of symmetry. Therefore, it can be used effectively to estimate P and S wave propagation velocities in orthorhombic media from surface seismic data with relative small maximum offset and for VSP geometries.

Finally, this work has been structured in the following manner. In Section 2 the formulation of the optimization problem, when the axis of symmetry is vertical, and also the generalized optimization problem, when the axis of symmetry forms an angle with respect to the vertical, is presented. In Section 3, we show that under some conditions, if the generalized optimization problem has a minimum, the minimum is global. In section 4 we present a brief description of the GSG method when applied to the proposed problem. The numerical results showing the performance of the algorithm are presented in Section 5. In Section 6 we present some conclusions.

2 General Optimization Problem

In this section we formulate the problem of tracing rays from a fixed source to a fixed receiver as the solution of an optimization problem in the same way Mao and Stuart (1997) and Cores *et al.* (2000) presented in their papers. The authors trace rays in a heterogeneous medium based on Fermat's principle and they consider the segment of a ray between any two consecutive interfaces a straight line. So, the trajectory of a ray for a pair of source-receptor (X_s, X_r) reflecting in the n^{th} layer is a piecewise linear path crossing $n+1$ interfaces. Therefore, the optimization problem is given by

$$\begin{array}{ll} Minimize & T_{X_s}^{X_r}(X,Y,Z) = \sum_{i=2}^{2n+1} \frac{l_i(X,Y,Z)}{v_i(X,Y,Z)}, \\ (X,Y,Z) \in \mathbb{R}^{3\times(2n-1)} & \end{array} \tag{1}$$

where

$$\begin{array}{rcl} l_i & = & \sqrt{(x_i - x_{i-1})^2 + (y_i - y_{i-1})^2 + (z_i - z_{i-1})^2}, \\ X_s & = & (x_1, y_1, z_1)^T, \\ X_r & = & (x_{2n+1}, y_{2n+1}, z_{2n+1})^T, \\ X & = & (x_2, ..., x_{2n})^T, \\ Y & = & (y_2, ..., y_{2n})^T, \\ Z & = & (z_2, ..., z_{2n})^T, \end{array} \tag{2}$$

(x_i,y_i,z_i) are the coordinates of the ray at the interfaces, $i = 1, \ldots, 2n+1$; v_i is the velocity of the layer delimited by by the $(i-1)^{th}$ and i^{th} interfaces, and it satisfies $v_i = v_{3+2n-i}$ for $i = 2, \ldots, n+1$ in the case of non-converted waves; otherwise, the down going velocities v_i, $i = 2, \ldots, n+1$, are different from the up going velocities v_i, $i = n+2, \ldots, 2n+1$ (see Figure 1).

The z_i coordinates depend on the ray trajectory points (x_i, y_i) in the following way, $z_i = f_i(x_i, y_i)$, for $i = 1, \ldots, 2n+1$, where any i^{th} interface function, f_i, for $i = 1, \ldots, n+1$ is obtained by biharmonic splines, Sandwell (1987). Moreover, $f_i = f_{2n-i+2}$ for $i = n+2, \ldots, 2n+1$ and, the $(n+1)^{th}$ interface, f_{n+1}, corresponds to the reflecting interface (see Figure 1).

2.1 Vertical axis of symmetry

In order to trace rays in anisotropic media we need to write the expression for the group velocities v_i, in the optimization problem (1). In this work we propose to use the 3-D ellipsoidal approximation of the group velocity for vertical axis of symmetry obtained by Contreras *et al.* (1997), which is given by:

$$\frac{1}{(v_i)^2} = \frac{1}{((v_{Z,j})_i)^2} \cos^2(\phi_{1_i}) + \frac{1}{((v_{NMO_{[XZ],j}})_i)^2} \cos^2(\phi_{2_i}) \sin^2(\phi_{1_i})$$

$$+ \quad \frac{1}{((v_{NMO_{[YZ],j}})_i)^2} \sin^2(\phi_{2_i}) \sin^2(\phi_{1_i}) \tag{3}$$

where, the index j indicates the wave propagation mode, i.e, $j = P$ means P-wave, and the splitting of the S-wave in anisotropic media is denoted by $j = SV$ and $j = SH$; $(v_{NMO_{[xz],j}})_i$ is the corresponding group normal move out velocity on the symmetry plane $[XZ]$ for the layer delimited by the $(i-1)^{th}$ interface and i^{th} interface, and

$$\begin{aligned}
\frac{1}{((v_{Z,P})_i)^2} &= C_{33}, \\
\frac{1}{((v_{NMO_{[XZ],P}})_i)^2} &= C_{55} + \frac{(C_{13}+C_{55})^2}{C_{33}-C_{55}}, \\
\frac{1}{((v_{NMO_{[YZ],P}})_i)^2} &= C_{44} + \frac{(C_{23}+C_{44})^2}{C_{33}-C_{44}}, \\
\frac{1}{((v_{Z,SV})_i)^2} &= C_{44}, \\
\frac{1}{((v_{NMO_{[XZ],SV}})_i)^2} &= C_{66}, \\
\frac{1}{((v_{NMO_{[YZ],SV}})_i)^2} &= C_{22} + \frac{(C_{23}+C_{44})^2}{C_{44}-C_{33}}, \\
\frac{1}{((v_{Z,SH})_i)^2} &= C_{55}, \\
\frac{1}{((v_{NMO_{[XZ],SH}})_i)^2} &= C_{11} + \frac{(C_{55}+C_{13})^2}{C_{55}-C_{33}}, \\
\frac{1}{((v_{NMO_{[YZ],SH}})_i)^2} &= C_{66},
\end{aligned} \tag{4}$$

the parameters C_{kl} are the elastic constants, ϕ_{1i} and ϕ_{2i} correspond to the polar group angle and the azimuthal group angle respectively in the layer delimited by the $(i-1)^{th}$ and i^{th} interfaces (see Figure 2).

The expression (3) was obtained by Contreras *et al.* (1997) by computing the eigenvalues of the Christoffel equation for orthorhombic media assuming small polar phase angle and utilizing a 3-D extension of the Levin (1978), Byun (1982) and Muir (1990) transformation, since the corresponding phase velocities on the symmetry planes for the different waves propagation modes are ellipsoidals under these assumptions.

On the other hand, in order to simplify the number of parameters on equation (3), it is clear from Figure 2 that:

$$
\begin{aligned}
\cos(\phi_{1_i}) &= \frac{f_i(x_i, y_i) - f_{i-1}(x_{i-1}, y_{i-1})}{l_i}, \\
\sin(\phi_{1_i}) &= \frac{\sqrt{(x_i - x_{i-1})^2 + (y_i - y_{i-1})^2}}{l_i}, \\
\cos(\phi_{2_i}) &= \frac{x_i - x_{i-1}}{\sqrt{(x_i - x_{i-1})^2 + (y_i - y_{i-1})^2}}, \\
\sin(\phi_{2_i}) &= \frac{y_i - y_{i-1}}{\sqrt{(x_i - x_{i-1})^2 + (y_i - y_{i-1})^2}},
\end{aligned}
$$

therefore, the group velocity, equation (3), can be written as a function of the ray trajectory coordinates (x_i, y_i, z_i), for $i = 1, 2, \ldots, 2n+1$ and $j = P, SV, SH$ (wave propagation modes) as follows:

$$
\frac{1}{v_i} = \frac{1}{l_i}\sqrt{\frac{(\Delta z_i)^2}{((v_{Z,j})_i)^2} + \frac{(\Delta x_i)^2}{((v_{NMO_{[XZ]},j})_i)^2} + \frac{(\Delta y_i)^2}{((v_{NMO_{[YZ]},j})_i)^2}}, \tag{5}
$$

where

$$
\begin{aligned}
\Delta x_i &= x_i - x_{i-1}, \\
\Delta y_i &= y_i - y_{i-1}, \\
\Delta z_i &= f_i - f_{i-1}.
\end{aligned}
$$

Introducing the expression of the group slowness approximation (5) in the travel time function given by (1), we have that our optimization problem in a 3-D ellipsoidal anisotropic media is given by

$$
\text{Min} \;\; T_{X_s}^{X_r}(X, Y, Z) = \sum_{i=2}^{2n+1} \sqrt{\frac{(\Delta z_i)^2}{((v_{Z,j})_i)^2} + \frac{(\Delta x_i)^2}{((v_{NMO_{[XZ]},j})_i)^2} + \frac{(\Delta y_i)^2}{((v_{NMO_{[YZ]},j})_i)^2}}. \tag{6}
$$

Therefore, for small polar phase angle and vertical axis of symmetry, the travel time function in (6) for P and S wave propagation modes is an ellipsoidal approximation of the travel time in orthorhombic media. Moreover, the unknown parameters of the problem (6) are only the vectors X and Y since all the components of vector Z can be expressed as a function of the components of X and Y. In the next section, we will obtain a more general equation for the travel time function, when the axis of symmetry is not vertical, as Michelena (1993) presents for a 2-D transversely isotropic media.

2.2 Non-vertical axis of symmetry

Now we suppose that the orientation of the axis of symmetry is not vertical. Then we extend the 2-D approach used by Michelena (1993) to obtain a 3-D ellipsoidal expression for the group slowness and the travel time function.

In order to find the travel time function, in this general case, we need to know the polar and azimuthal rotation angles that allow us to rotate the coordinate system corresponding to the non vertical axis of symmetry, let's say, $o(X^{'}, Y^{'}, Z^{'})$, to the coordinate system associated to the vertical axis of symmetry, $o(X, Y, Z)$ (See Figure 3). Let Ψ be the azimuthal rotation angle (i.e., the angle between X and the projection of $Z^{'}$ on the plane $[XY]$, measured counterclockwise) and Θ the polar rotation angle (i.e., the angle between the vertical axis Z, and $Z^{'}$, measured clockwise). Regardless of the symmetry axis, we can assume or force without loss of generality that the projection of $X^{'}$ on the plane $[XY]$ coincides with the projection of $Z^{'}$ on the plane $[XY]$, as it appears in Figure 3. Then, it is sufficient to rotate (clockwise) $X^{'}$ an angle Ψ so that $X^{'}$ and X belong to the same plane. Additionally we obtain that $Y^{'}$ and Y are also in the same plane. Now, we only need to perform a rotation Θ (counterclockwise), to locate $Z^{'}$ over the vertical axis Z. The application of these rotations respectively will allow us to get the generalized travel time equation for any axis of symmetry in an anisotropic medium. These rotations can be represented by the following matrices:

$$R_{Azimuthal} = \begin{pmatrix} \cos(\Psi) & \sin(\Psi) & 0 \\ -\sin(\Psi) & \cos(\Psi) & 0 \\ 0 & 0 & 1 \end{pmatrix} \quad \text{and,} \tag{7}$$

$$R_{Polar} = \begin{pmatrix} \cos(\Theta) & 0 & -\sin(\Theta) \\ 0 & 1 & 0 \\ \sin(\Theta) & 0 & \cos(\Theta) \end{pmatrix}. \tag{8}$$

Let us denote the distance segment between two consecutive points, in the ray trajectory on the layer delimited by the $(i-1)^{th}$ and i^{th} interfaces by $(\Delta x_i, \Delta y_i, \Delta z_i)$, in the coordinate system $o(X, Y, Z)$, and by $(\Delta x_i^{'}, \Delta y_i^{'}, \Delta z_i^{'})$ in the coordinate system $o(X^{'}, Y^{'}, Z^{'})$. Also denote by Θ_i and Ψ_i the polar and azimuthal rotation angles corresponding to the layer i, which satisfy $\Theta_i = \Theta_{3+2n-i}$ and $\Psi_i = \Psi_{3+2n-i}$ for $i = 2, \ldots, n+1$. Hence, in a 3-D homogeneous ellipsoidal anisotropic medium with any axis of symmetry, we can express $(\Delta x_i^{'}, \Delta y_i^{'}, \Delta z_i^{'})$ in the old coordinate system, $o(X, Y, Z)$, as follows:

$$\begin{pmatrix} \Delta x_i^{'} \\ \Delta y_i^{'} \\ \Delta z_i^{'} \end{pmatrix} = R_{Polar} R_{Azimuthal} \begin{pmatrix} \Delta x_i \\ \Delta y_i \\ \Delta z_i \end{pmatrix}, \tag{9}$$

that is,

$$\begin{aligned}
\Delta x_i^{'} &= \Delta x_i \cos(\Theta_i)\cos(\Psi_i) + \Delta y_i \sin(\Psi_i)\cos(\Theta_i) - \Delta z_i \sin(\Theta_i), && (10)\\
\Delta y_i^{'} &= -\Delta x_i \sin(\Psi_i) + \Delta y_i \cos(\Psi_i), && (11)\\
\Delta z_i^{'} &= \Delta x_i \cos(\Psi_i)\sin(\Theta_i) + \Delta y_i \sin(\Theta_i)\sin(\Psi_i) + \Delta z_i \cos(\Theta_i), && (12)
\end{aligned}$$

Therefore, in this work, we propose to trace rays in 3-D ellipsoidal anisotropic media with tilted axis of symmetry by solving the following unconstrained optimization problem

$$\text{Min} \;\; T_{X_s}^{X_r}(X,Y,Z) = \sum_{i=2}^{2n+1} \sqrt{\frac{(\Delta z_i^{'})^2}{((v_{Z,j})_i)^2} + \frac{(\Delta x_i^{'})^2}{((v_{NMO_{[XZ]},j})_i)^2} + \frac{(\Delta y_i^{'})^2}{((v_{NMO_{[YZ]},j})_i)^2}}. \quad (13)$$

First, observe that it does not matter the sign of Θ_i and Ψ_i (clockwise or counterclockwise) if we apply the corresponding rotation matrices in the right way (i.e., in the reverse measured mode).

We have that problem (13) is a generalized travel time formulation, for any wave propagation mode, since:

1. It is clear from equation (13) that for $\Theta_i = 0$, $\Psi_i = 0$, and $((v_{Z,j})_i) = ((v_{NMO_{[XZ]},j})_i) = ((v_{NMO_{[YZ]},j})_i) = \text{constant}$, equation (13) is the exact travel time function in an 3-D isotropic homogeneous medium, as the one used by Mao and Stuart (1997) and Cores *et al.* (2000).

2. We have that for $\Psi_i = 0$,

$$\begin{aligned}
\Delta x_i^{'} &= \Delta x_i \cos(\Theta_i) - \Delta z_i \sin(\Theta_i), && (14)\\
\Delta z_i^{'} &= \Delta x_i \sin(\Theta_i) + \Delta z_i \cos(\Theta_i). && (15)
\end{aligned}$$

   which correspond to the travel time in 2-D homogeneous elliptically anisotropic media with tilted axis of symmetry given by Michelena (1993) for a 2-D transversely isotropic medium.

3. Equation (13) generalizes to 3-D ellipsoidal anisotropic media the results obtained by Michelena (1993) for a 2-D elliptical anisotropic medium (which is clear from the previous comment). Moreover, near to the vertical, equation (13) is a precise approximation in orthorhombic media.

4. Finally, equation (6) can be attained from equation (13) just considering $\Theta_i = 0$ and $\Psi_i = 0$.

Therefore, close to the vertical, equation (13) is a generalized travel time expression in anisotropic media, since it is a good travel time approximation in homogeneous transversely isotropic media and homogeneous orthorhombic media with tilted axis of symmetry, depending on the input model parameters.

3 Global Minimum

In this section we present the model conditions that allow us to prove that any solution of the generalized 3-D ellipsoidal anisotropic ray tracing problem (13) is a global minimum. A similar result was shown in Cores *et al.* (2000) for the case of tracing rays using Fermat's principle and assuming straight ray segments between layers in an isotropic homogeneous medium.

First, to simplify the computations we denote:

$$\lambda_{1i} = \frac{1}{(v_{NMO_{[XZ]},j})_i}, \quad \lambda_{2i} = \frac{1}{(v_{NMO_{[YZ]},j})_i} \quad \text{and} \quad \lambda_{3i} = \frac{1}{(v_{Z,j})_i},$$

Then the travel time function (13) is given by

$$T_{X_s}^{X_r}(X,Y,Z) = \sum_{i=2}^{2n+1} \|(\lambda_{1i}h_{1i}(X,Y,Z), \lambda_{2i}h_{2i}(X,Y,Z), \lambda_{3i}h_{3i}(X,Y,Z))\|_2 \qquad (16)$$

where,

$$\begin{aligned}
h_{1i}(X,Y,Z) &:= \Delta x_i^{'} = \delta_{1i}\Delta x_i + \delta_{2i}\Delta y_i - \delta_{3i}\Delta z_i, && (17)\\
h_{2i}(X,Y,Z) &:= \Delta y_i^{'} = -\gamma_{1i}\Delta x_i + \gamma_{2i}\Delta y_i, && (18)\\
h_{3i}(X,Y,Z) &:= \Delta z_i^{'} = \epsilon_{1i}\Delta x_i + \epsilon_{2i}\Delta y_i + \epsilon_{3i}\Delta z_i, && (19)
\end{aligned}$$

are continuously differentiable functions from $\mathbb{R}^{6n-3}$ to $\mathbb{R}$ and,

$$\begin{aligned}
\delta_{1i} &= \cos(\Theta_i)\cos(\Psi_i),\\
\delta_{2i} &= \cos(\Theta_i)\sin(\Psi_i),\\
\delta_{3i} &= \sin(\Theta_i),\\
\gamma_{1i} &= \sin(\Psi_i),\\
\gamma_{2i} &= \cos(\Psi_i),\\
\epsilon_{1i} &= \cos(\Psi_i)\sin(\Theta_i),\\
\epsilon_{2i} &= \sin(\Theta_i)\sin(\Psi_i),\\
\epsilon_{3i} &= \cos(\Theta_i),
\end{aligned}$$

are given constants. For the purpose of this section it is sufficient to show that the objective function in (13) is convex, since the travel time function with vertical axis of symmetry, given in problem (6), is a particular case of the general problem (13). In fact, we can get problem (6) from problem (16) by taking $\Theta_i = \Psi_i = 0^o$ which is the same as considering, $\delta_{2i} = \delta_{3i} = \gamma_{1i} = \epsilon_{i1} = \epsilon_{2i} = 0$ and $\delta_{1i} = \gamma_{2i} = \epsilon_{3i} = 1$.

The following Lemma will be used to prove that the general travel time formulation,

given in problem (13) is a convex problem.

Lemma 3.1
The functions defined by (17), (18) and (19) are convex functions for a dip or stratified model (*i.e.*, $z_i = f_i(x, y) = a_i x_i + b_i y_i + c_i$).

Proof:
It is clear that we only need to prove the result for h_{1i} or h_{3i} since they have the same form. On the other hand, function h_{2i} is a linear function and does not depend on Z, so it is convex independently of the component values of the vector Z. Let (X, Y, Z) and (U, V, W) be any vectors in $\mathbb{R}^{6n-3}$, $B = \alpha(X, Y, Z) + (1 - \alpha)(U, V, W)$, and for all $\alpha \in [0, 1]$ we have that,

$$\begin{aligned} h_{1i}(B) &= \delta_{1i}(\alpha\Delta x_i + (1-\alpha)\Delta u_i) + \delta_{2i}(\alpha\Delta y_i + (1-\alpha)\Delta v_i) + \\ &- \delta_{3i}(\alpha(a_i x_i + b_i y_i + c_i) + (1-\alpha)(a_i u_i + b_i v_i + c_i) + \\ &- \alpha(a_{i-1} x_{i-1} + b_{i-1} y_{i-1} + c_{i-1}) - (1-\alpha)(a_{i-1} u_{i-1} + b_{i-1} v_{i-1} + c_{i-1})) \\ &= \alpha(\delta_{1i}\Delta x_i + \delta_{2i}\Delta y_i - \delta_{3i}\Delta z_i) + (1-\alpha)(\delta_{1i}\Delta u_i + \delta_{2i}\Delta v_i - \delta_{3i}\Delta w_i) \\ &= \alpha h_{1i}(X, Y, Z) + (1-\alpha) h_{1i}(U, V, W) \end{aligned}$$

Therefore, function h_{1i} is convex and so is h_{3i}.

Theorem 3.1
The objective function in problem (13) is convex for a dip or stratified model (i.e., $z_i = f_i(x_i, y_i) = a_i x_i + b_i y_i + c_i$) with constant components of the velocity in the layers (homogeneous 3-D ellipsoidal anisotropic medium).

The proof follows directly since the functions h_{1i}, h_{2i} and h_{3i} are convex functions, and the travel time function in problem (13), rewritten as (16), is the sum of Euclidean vector norms of convex functions.

From this result we can conclude that for stratified and dip 3-D homogeneous ellipsoidal anisotropic media it does not make any sense to think about global optimization (that finds the smallest minimum), since the objective function is convex so, any solution of problem (6) or problem (13) is the global minimum. Therefore, problems (6) and (13) are not only a simple formulation for tracing rays in anisotropic media with any axis of symmetry but also a formulation that gives the optimal rays in the medium. Hence any global deterministic optimization algorithm, in the sense that convergence is attained from any initial guess, will find the solution of the problem.

In the next section we explain the main steps in the GSG method and the advantages of solving problem (13) or problem (6) by the GSG optimization strategy.

4 Numerical Optimization Approach

The global spectral gradient (GSG) method is a low cost and low storage technique that requires few floating point operations and first order information as we mentioned in the previous sections. Also it is known that the ray tracing problem is time consuming even with recent computational technology. Moreover, the GSG method was used for tracing rays in heterogeneous isotropic 2-D and 3-D media bringing enormous computational advantages, Cores *et al.* (2000). For those reasons, in this work we apply the spectral gradient (SG) method for solving the proposed generalized 3-D ellipsoidal anisotropic ray tracing (13). Additionally, the formulation presented in this work involves a convex travel time function so, any stationary point found by the GSG method is a global minimum, if the model is an homogeneous stratified or dipping ellipsoidal anisotropic medium. The convexity and simplicity of the formulation together with the computational advantages of the method makes the strategy proposed in this work a very efficient and fast strategy for tracing rays in orthorhombic media.

The iterates of the SG method, Raydan (1997), are defined as in the classical gradient method,

$$X_{k+1} = X_k + \alpha_k d_k, \tag{20}$$

where $d_k = -\nabla T_{X_s}^{X_r}(X_k)$, and $X_k \in \mathbb{R}^{4n-2}$ corresponds to the vectors X and Y, defined in (2), at iteration k. The crucial difference between the classical steepest descent method and the SG method is the choice of the step length α_k. In the SG method the step length is computed by

$$\alpha_k = \frac{s_{k-1}^T s_{k-1}}{s_{k-1}^T y_{k-1}} \tag{21}$$

where,

$$\begin{aligned} s_{k-1} &= X_k - X_{k-1} \quad \text{and} \\ y_{k-1} &= \nabla T_{X_s}^{X_r}(X_k) - \nabla T_{X_s}^{X_r}(X_{k-1}). \end{aligned}$$

Then with this choice of the step length the SG method is not a classical descent method but the convergence of the method can be accelerated. Moreover, GSG method uses a globalization strategy that consists in utilizing a non monotone line search scheme that allows the function to increase at some iterations to maintain the good properties of the SG method. This strategy consists of verifying the following condition,

$$T_{X_s}^{X_r}(X_k + \alpha_k d_k) \leq \max_{0 \leq j \leq M-1} T_{X_s}^{X_r}(X_{k-j}) - \gamma \alpha_k \nabla T_{X_s}^{X_r}(X_k)^T \nabla T_{X_s}^{X_r}(X_k), \tag{22}$$

where M is a positive constant given by the user and $\gamma \in (0, 1)$ is also given . This condition forces the function to decrease at least every M iterations and guarantees

convergence from any initial iterate. On the other hand, it is clear that forcing condition (22) does not imply as many function evaluations as an exhaustive classical line search strategy (Armijo-type condition).

5 Numerical Results

Here we illustrate the effect of considering a 3-D ellipsoidal anisotropic medium with tilted axis of symmetry. We solve problem (13) for different values of the polar and azimuthal rotation angles, Θ_i and Ψ_i, to see the effect of the anisotropy in the ray trajectory and in the reflection points of the ray trajectory. We also show the computational advantages of GSG method by comparing it with the classical Steepest Descent method (SD) for solving the ray tracing problem (13).

Model 1

First, we consider an anisotropy model of one flat layer with one source at $(6, 6, 0)$ and 181 receivers located uniformly distributed in a radius of 2 kilometers from the source. The layer is located at 1 kilometer from the surface.

Model 2

We also consider a 3D synthetic orthorhombic medium with vertical axis of symmetry consisting of one source at $(0, 0, 0)$ and 157 receivers at the surface, $z = 0$, where the x coordinates are 17 m apart and the y coordinates are generated by random. The model has five dipping layers where P-S converted wave velocities are considered.

We design four different tests on both models, where three of them are based on Model 1.

Test1: First, we run the ray tracing code for Model 1 and we vary the azimuthal angle, Ψ_i, from 0^o to 180^o and the polar angle, Θ_i, from 0^o to 180^o for non-converted waves.

Test 2: Second, we consider Model 1 and we run the program for $0^o \leq \Theta_i \leq 180^o$ and $0^o \leq \Psi_i \leq 180^o$ for converted waves.

For these two tests, the components of the velocity for the non-converted case satisfy, for $i = 2$ $(n = 1)$,

$$(V_{Z,j})_i \geq (V_{NMO_{[YZ]},j})_i \geq (V_{NMO_{[XZ]},j})_i, \quad \text{for} \quad j = P \tag{23}$$

and for the converted case, satisfy (23), for $j = P, S$, and also satisfy for $i = 2$ $(n = 1)$,

$$\begin{aligned} (V_{Z,P})_{n-i+3} &\geq (V_{Z,S})_{n+i}, \\ (V_{NMO_{[YZ]},P})_{n-i+3} &\geq (V_{NMO_{[YZ]},S})_{n+i}, \\ (V_{P,NMO_{[XZ]},P})_{n-i+3} &\geq (V_{NMO_{[XZ]},S})_{n+i}. \end{aligned} \tag{24}$$

Moreover, for the first two test the values of the components of the velocity for non-converted waves are:

$$(v_{NMO_{[XZ]},P})_2 = 3000 \text{ m/s},$$

$$\begin{aligned} (v_{NMO_{[YZ],P}})_2 &= 5000 \text{ m/s}, \\ (v_{Z,P})_2 &= 7000 \text{ m/s}. \end{aligned} \tag{25}$$

In the case of converted waves we consider the same values for the components of the P-wave velocity, which are given (25) and the values of the S-wave components of the velocity are:

$$\begin{aligned} (v_{NMO_{[xz],S}})_3 &= 1000 \text{ m/s}, \\ (v_{NMO_{[yz],S}})_3 &= 3000 \text{ m/s}, \\ (v_{Z,S})_3 &= 5000 \text{ m/s}. \end{aligned} \tag{26}$$

The velocities in equations (25) and (26) correspond to consider elastic constants, $C_{11} = 0.25$, $C_{12} = 0.02$, $C_{13} = -0.1079$, $C_{22} = 0.1112$, $C_{32} = -0.0392$, $C_{33} = 0.0204$, $C_{44} = 0.04$, $C_{55} = 0.1111$ and $C_{66} = 1$ in equations given by (4).

Test 3: We consider Model 1 and we vary the polar and azimuthal angle for values of the velocity components that not satisfy equations (23) or (24) for some $i = 2, \ldots, n+1$.. Those values are given by

$$\begin{aligned} (v_{NMO_{[XZ],P}})_2 &= 7000 \text{ m/s}, \\ (v_{NMO_{[YZ],P}})_2 &= 2500 \text{ m/s}, \\ (v_{Z,P})_2 &= 3000 \text{ m/s}, \end{aligned} \tag{27}$$

$$\begin{aligned} (v_{NMO_{[XZ],S}})_3 &= 2000 \text{ m/s}, \\ (v_{NMO_{[YZ],S}})_3 &= 1000 \text{ m/s}, \\ (v_{Z,S})_3 &= 5000 \text{ m/s}. \end{aligned} \tag{28}$$

Test 4: The final test consists in computing all ray trajectories for Model 2 considering converted wave and different axis of symmetry using the GSG method and the classical SD method, for which a standard Armijo-type line search procedure is used for obtaining the step length, see Dennis Jr. and Schnabel (1983). Then, in order to illustrate the speed of convergence and the computational properties of the GSG method, we compare the computational work and CPU time for both schemes when solving problem (13). This comparison is fair since both methods are similar, they differ only in the choice of the step length (α_k). Moreover, the classical SD method is well known and it has been utilized for many authors in geophysics, for example Luo and Schuster (1991) and Gauthier *et al.* (1986) among others. The velocities in this test are given by

$$\begin{aligned} (v_{Z,P})_i &= 1500 + 100 * i \text{ m/s}, \\ (v_{NMO_{[XZ],P}})_i &= 1200 + 50 * i \text{ m/s}, \quad \text{for} \quad i = 2, \ldots, n+1 \\ (v_{NMO_{[YZ],P}})_i &= 1350 + 80 * i \text{ m/s}, \end{aligned}$$

and

$$\begin{aligned}
(v_{Z,S})_{n+i} &= 1400 + 100 * (n + 3 - i) \ \text{m/s}, \\
(v_{NMO_{[XZ]},S})_{n+i} &= 1000 + 50 * (n + 3 - i) \ \text{m/s}, \quad \text{for} \quad i = 2, \ldots, n + 1 \\
(v_{NMO_{[yz]},S})_{n+i} &= 1150 + 80 * (n + 3 - i) \ \text{m/s}.
\end{aligned}$$

It is clear that these values of the velocity components satisfy equations (24) and (23), but the proposed approach works independently of the order relation in the velocities.

All test were run on a SUN Station ULTRA 5, with 128 Mg of Ram, using Fortran 77. The stopping criterion for GSG and SD method is

$$\|\nabla T_{X_s}^{X_r}(X_k)\| \leq 0.5 \times 10^{-6}(1 + |T_{X_s}^{X_r}(X_k)|),$$

and the value of the parameter M for the GSG method is 8. In the numerical results we use the following notation, for example; **Azimuthal-30** means no vertical axis of symmetry where the azimuthal rotation angle $\Psi = 30^0$; **Polar-30** means no vertical axis of symmetry where the polar rotation angle is given by $\Theta = 30^o$ and; **Azimuthal-45, Polar-30** means that $\Theta = 30^o$ and $\Psi = 45^o$ with axis of symmetry non vertical. Moreover, since we can trace rays considering converted wave or non converted waves we denote by **P-P** when non converted waves are used in the problem, and we denote by **P-S** when converted waves are considered in the problem.

All Figures from 6 through 12 show part of the ray trajectories from the source to the reflection point (left figures) and the projection of this part of the trajectories on the flat layer (right figures). In order to understand the behavior of the approximation, we will consider a variety of values of the rotation angles and different values of the NMO velocities on the symmetry planes, which are given by equations (25), (26), (27) and (28). The projection of the source on the flat layer is the point $(6, 6)$, that from now on we refer to it as the center point.

Figure 4 shows the trajectory of the rays corresponding to Model 1 for non-converted waves and vertical axis of symmetry when the components of the velocity are constants and given by (25) (i.e., the medium is homogeneous and ellipsoidal anisotropic). Figure 5 shows the projection of the down going rays corresponding to Figure 4 on the flat layer. For Model 1 with vertical symmetry axis and non-converted waves, it can be mathematically shown that the reflection points must be uniformly located on the flat layer in a circle of radius 1 km and center $(6, 6)$, as Figure 5 illustrates. So, the reflection points in this case coincide with the ones obtained for a homogeneous isotropic medium, which corresponds to taking $(V_{Z,P})_i = (V_{NMO_{[YZ]},P})_i = (V_{NMO_{[XZ]},P})_i = constant$, for $i = 2, \ldots, n + 1$. However, associated travel times do not coincide with the ones obtained in a 3-D homogeneous isotropic medium unless the NMO velocities along the symmetry planes are the same.

The results for the Test 1 are given by Figures 6, 7 and 8. From those figures we can see that the projection of the ray trajectories on the plane $[XY]$ form a circle, since the down going and up going components of the velocity are the same. This fact can be easily proved for $\Theta_i = \Psi_i = 0^o$. We also observe that the projection of the ray trajectories in Figure 6 is symmetric with respect to the center point as it was in Figure 5. Moreover, the x and y coordinates of the reflection points correspond to the middle points between X_s and X_r, since for non converted waves, the azimuthal rotation does not change the reflection points associated to a homogeneous isotropic medium, even though the associated travel times are different from the ones obtained in a homogeneous isotropic medium. Indeed in Figure 6, $\Theta_2 = \Theta_3 = 0^o$, $\Psi_2 = \Psi_3 \neq 0^o$, and therefore,

$$\begin{aligned}
\Delta x_2^{'} &= \Delta x_2 \cos(\Psi_2) + \Delta y_2 \sin(\Psi_2), \\
\Delta y_2^{'} &= -\Delta x_2 \sin(\Psi_2) + \Delta y_2 \cos(\Psi_2), \\
\Delta z_2^{'} &= \Delta z_2, \\
\Delta x_3^{'} &= \Delta x_3 \cos(\Psi_3) + \Delta y_3 \sin(\Psi_3), \\
\Delta y_2^{'} &= -\Delta x_3 \sin(\Psi_3) + \Delta y_3 \cos(\Psi_3), \\
\Delta z_3^{'} &= \Delta z_3.
\end{aligned}$$

Then the reflecting point in a homogeneous isotropic medium, that is,

$$(x_2, y_2, z_2) = (\frac{x_1 + x_3}{2}, \frac{y_1 + y_3}{2}, z_2), \tag{29}$$

is also a solution of the problem (13) for Figure 6, in a homogeneous ellipsoidal anisotropic medium, since:

$$\begin{aligned}
\Delta x_2 &= \Delta x_3, \\
\Delta y_2 &= \Delta y_3, \\
\Delta z_2 &= -\Delta z_3, \text{and} \\
(v_{Z,j})_2 &= (v_{Z,j})_3, \\
(v_{NMO_{[XZ],j}})_2 &= (v_{NMO_{[XZ],j}})_3, \\
(v_{NMO_{[YZ],j}})_2 &= (v_{NMO_{[YZ],j}})_3,
\end{aligned}$$

which implies that,

$$(\Delta x_2^{'})^2 = (\Delta x_3^{'})^2, (\Delta y_2^{'})^2 = (\Delta y_3^{'})^2, \text{and} (\Delta z_2^{'})^2 = (\Delta z_3^{'})^2, \tag{30}$$

and therefore, $\nabla T_{X_s}^{X_r} = 0$ (see Appendix A). Thus, we can conclude from Theorem 3.1 that (x_2, y_2, z_2) given by (29) is the unique global solution of the problem for Test 1 (Figure 6).

However, if only a polar rotation occurs (Figure 7), then the center point is not the center of the projection circle as before, since the equations given in (30) are no longer true. The location of the center point is on the line $y = 6$ and depends on the polar rotation angle. Moreover, if both angles are different from zero, Figure 8, we observe that the center point is not even on the line $y = 6$ since an azimuthal rotation was performed and its location will depend on both angles.

The results for Test 2 are illustrated in Figures 9, 10 and 11. In this test we consider converted waves and then it seems natural that the ray trajectory projections form an "ellipse", because of the properties (23) and (24) of the velocity components. In this case we expect to see the effects of the azimuthal rotation angle since we have converted waves. Moreover, if only an azimuthal rotation angle is performed (Figure 9) the center point corresponds to the center of the "ellipse" but the "ellipse" is rotated Ψ degrees counterclockwise, as it was expected. On the other hand, if only a polar rotation angle occurs (Figure 10) the ray trajectory projections also form an "ellipse" with center different from the center point $(6, 6)$. The location of the center point is on the line $y = 6$, and its location depends on the value of the polar rotation angle, as in Test 1. We can also observe from Figure 10 that for $\Theta = 90^o$, the "ellipse" is now vertical because the properties (23) and (24) imply that the biggest axis of the "ellipse" becomes the smallest and vice versa. Finally, Figure 11 illustrates the results when both angles are different from zero at the same time. Those results clearly indicate the same behavior of the non-converted case. Indeed, the center point is not the center of the "ellipse" because of the polar rotation angle and the fact that the "ellipse" is rotated Ψ degrees counterclockwise.

Figure 12 shows the results for Test 3. In this figure we observe that the ray projections form a figure that is not an "ellipse" as in Test 2. The shape of the ray trajectory projections will depend on the values of the NMO velocities on the symmetry planes. Moreover, the effect of the ellipsoidal anisotropy for different values of the azimuthal and polar rotation angles follow the same behavior of the previous tests, as we can see in Figure 12.

The results in Table 1 shows the average number of iterations (Δ_{iter}) and the total CPU time (Total CPU time) require for obtaining the 785 optimal ray trajectories in Test 4, for the GSG and SD methods when solving problem (13) from the same initial ray path. From these results is clear that the GSG method outperforms the SD method (in CPU time and computational work) for different values of the rotation angles Θ_i and Ψ_i with $i = 1, \ldots, 5$. Even though both methods use the same negative gradient direction, the SD method is a descent method at every iteration, in high contrast with the GSG method that is not a descent method. The basic and crucial difference is the spectral step length (α_k). This implies that the spectral choice of

the step length can speed up the convergence of the gradient type methods. So, the GSG method could be a very convenient method for large size non linear optimization problems, where first order information is available.

6 Conclusions

The generalized formulation (13) is a nonlinear convex ellipsoidal problem that gives the ray trajectories in 3-D homogeneous isotropic media, 2-D homogeneous elliptically anisotropic media, and 3-D homogeneous ellipsoidal media for converted waves, depending on the input parameters. Moreover, near the vertical or for small polar group angle, this ray tracing is an accurate technique for obtaining the rays in a 2-D homogeneous transversely isotropic media and in a 3-D homogeneous orthorhombic media. However, formulation (13) also works in an anisotropic heterogeneous medium where the heterogeneous model is described as a superposition of homogeneous anisotropic layers as Model 2.

The solution of optimization problem (13) by the GSG method gives the optimal ray trajectories (for homogeneous stratified or dipping models) in 3-D ellipsoidal anisotropic medium as a consequence of Theorem 3.1. Therefore, the simplicity of the formulation together with the low cost and storage GSG method makes the approach proposed in this work a global and efficient way to introduce anisotropy in a 3-D medium. Moreover, the travel time formulation developed in this work is a fast and accurate tool to model the travel time close to the axis of symmetry in an orthorhombic medium and to obtain P-P and P-S reflection times in media with tilted axis of symmetry. Therefore, it can be used effectively to estimate P and S wave propagation velocities in orthorhombic media from surface seismic data with relative small maximum offset and for VSP geometries.

Finally, the numerical results illustrate how the anisotropic affects the ray trajectory in the medium, in particular this approach allows us to know the location of the reflection points for different axis of symmetry. Moreover, from the results we found that even when the reflection points in a homogeneous isotropic and ellipsoidal anisotropic media are the same, the associated travel times are different.

References

Byun, B. S. 1982. Sismic parameters for media with elliptical velocities dependencies. *Geophysics*, **47,** 1621–1626.

Castillo, Z., Cores, D. and Raydan, M. 2000. Low cost optimization techniques for solving the nonlinear seismic reflection tomography problem. *Optimization Engineering*, **1,** 155–169.

Chapman, C. H. and Pratt, R. G. 1992. Traveltime tomography in anisotropic media-I. Theory:. *Geophysics J. Intl*, **109,** 1–19.

Contreras, P., Klie, H. and Michelena, R. J. 1997. Ellipsoidal approximation of velocities in orthorombic media. *Fifth international congress of the Brazilian geophysical society*, **1,** 255–258.

Cores, D., Fung, G. and Michelena, R. J. 2000. A fast and global low storage optimization technique for tracing rays in 2d and 3d isotropic media. *Journal of Applied Geophysics*, **45,** no. 4, 273–287.

D'Agosto, C., Donati, M. S. and Michelena, R. J. 1998. Tomography + pre-stack depth migration of P-S converted waves. 68th Annual International Meeting of the Soc. Expl. Geophys., Extended Abstracts, 1361-1364.

D'Agosto, C. and Michelena, R. J. 1997. Tomographic estimation of compressional and shear wave velocities from P-S converted waves. 67th Annual International Meeting of the Soc. Expl. Geophys., Extended Abstracts, 1885-1888.

Dennis Jr., J.E. and Schnabel, R.B. 1983. *Numerical Methods for Unconstrained Optimization and Nonlinear Equations*. Englewood Cliffs, NJ: Prentice-Hall.

Gauthier, O., Virieux, J. and Tarantola, A. 1986. Two-dimensional nonlinear inversion of seismic waveforms: Numerical results. *Geophysics*, **51,** 1387–1403.

Grechka, V. Y. and McMechan, G. A. 1996. 3-D two point ray tracing for heterogeneous weakly transversely isotropic media. *Geophysics*, **61,** 1883–1894.

Levin, F. K. 1978. The reflection refraction and difraction of waves in medis with elliptical velocity dependence. *Geophysics*, **43,** 528–537.

Luo, Y. and Schuster, G. T. 1991. Wave-equation traveltime inversion. *Geophysics*, **56,** no. 5, 645–653.

Mao, W. and Stuart, G. W. 1997. Rapid multi-wave-type ray tracing in complex 2d and 3d isotropic media. *Geophysics*, **62,** no. 1, 298–308.

Michelena, R. J. 1993. Anisotropic traveltime tomography. Ph.D Thesis, Department of Geophysics, Stanford University, California, United States of America.

Michelena, R. J., Muir, F. and Harris, J. M. 1993. Anisotropic traveltime tomography. *Geophys. Prosp.*, **41,** 381–412.

Muir, F. 1990. Various equations for TI media. Technical Report Technical Report SEP-70. Stanford University, California, United States of America.

Pratt, R. G. and Chapman, C. H. 1992. Traveltime tomography in anisotropic media-II. Application:. *Geophysics J. Intl*, **109,** 20–37.

Raydan, M. 1997. The Barzilai and Borwein gradient method for the large scale unconstrained minimization problem. *SIAM J. Opt.*, **7,** 26–33.

Sandwell, D. T. 1987. Biharmonic spline interpolation os geos-3 and seasat altimeter data. *Geophys. Research Letters*, **14,** no. 2, 139–142.

Thomsen, L. 1986. Weak elastic anisotropy. *Geophysics*, **51,** no. 6, 1954–1966.

Tsvankin, I. 1996. Effective parameters and p-wave velocity for orthorhombic anisotropy. 66th Ann. International Meeting, Soc. Expl. Geophys.

7 Appendix A

The gradient of the general travel time function,

$$\nabla T_{X_s}^{X_r} = \left(\frac{\partial T_{X_s}^{X_r}}{\partial x_2}, \ldots, \frac{\partial T_{X_s}^{X_r}}{\partial x_{2n}}, \frac{\partial T_{X_s}^{X_r}}{\partial y_2}, \ldots, \frac{\partial T_{X_s}^{X_r}}{\partial y_{2n}} \right)^T$$

where the partial derivatives for $i = 1, \ldots, 2n$ are given by

$$\begin{aligned}
\frac{\partial T_{X_s}^{X_r}}{\partial x_i} &= \frac{\Delta x_i^{'} R_i + \Delta y_i^{'} P_i + \Delta z_i^{'} H_i}{t_i} - \frac{\Delta x_{i+1}^{'} R_{i+1} + \Delta y_{i+1}^{'} P_{i+1} + \Delta z_{i+1}^{'} H_{i+1}}{t_{i+1}} \\
\frac{\partial T_{X_s}^{X_r}}{\partial y_i} &= \frac{\Delta x_i^{'} \hat{R}_i + \Delta y_i^{'} \hat{P}_i + \Delta z_i^{'} \hat{H}_i}{t_i} - \frac{\Delta x_{i+1}^{'} \hat{R_{i+1}} + \Delta y_{i+1}^{'} \hat{P_{i+1}} + \Delta z_{i+1}^{'} \hat{H_{i+1}}}{t_{i+1}}
\end{aligned}$$

and

$$\begin{aligned}
R_i &= \frac{\cos(\Theta_i)\cos(\Psi_i) - \frac{\partial f_i}{\partial x_i}\sin(\Theta_i)}{((v_{NMO_{[XZ],j}})_i)^2} \\
P_i &= \frac{-\sin(\Psi_i)}{((v_{NMO_{[YZ],j}})_i)^2} \\
H_i &= \frac{\sin(\Theta_i)\cos(\Psi_i) + \frac{\partial f_i}{\partial x_i}\cos(\Theta_i)}{((v_{Z,j})_i)^2} \\
\hat{R}_i &= \frac{\cos(\Theta_i)\sin(\Psi_i) - \frac{\partial f_i}{\partial y_i}\sin(\Theta_i)}{((v_{NMO_{[XZ],j}})_i)^2} \\
\hat{P}_i &= \frac{\cos(\Psi_i)}{((v_{NMO_{[YZ],j}})_i)^2} \\
\hat{H}_i &= \frac{\sin(\Theta_i)\sin(\Psi_i) + \frac{\partial f_i}{\partial y_i}\cos(\Theta_i)}{((v_{Z,j})_i)^2} \\
t_i &= \sqrt{\frac{(\Delta z_i^{'})^2}{((v_{Z,j})_i)^2} + \frac{(\Delta x_i^{'})^2}{((v_{NMO_{[XZ],j}})_i)^2} + \frac{(\Delta y_i^{'})^2}{((v_{NMO_{[YZ],j}})_i)^2}}
\end{aligned}$$

8 Figures

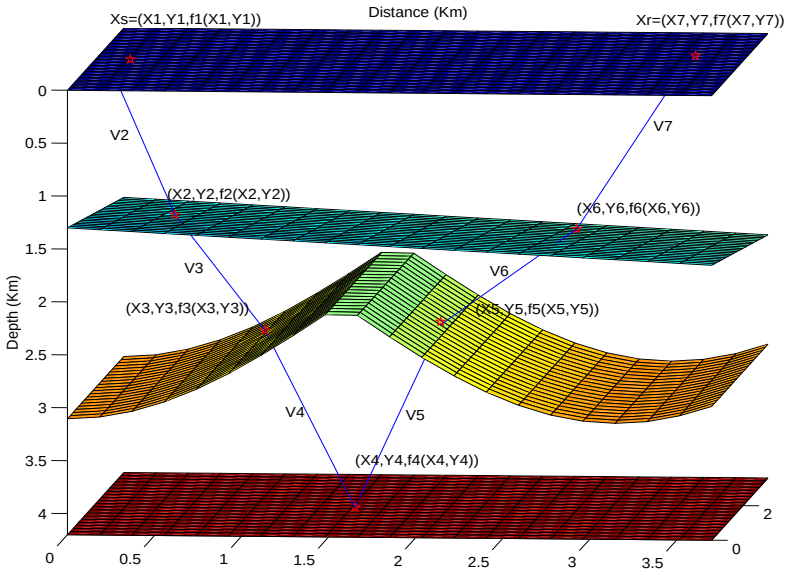


Figure 1:

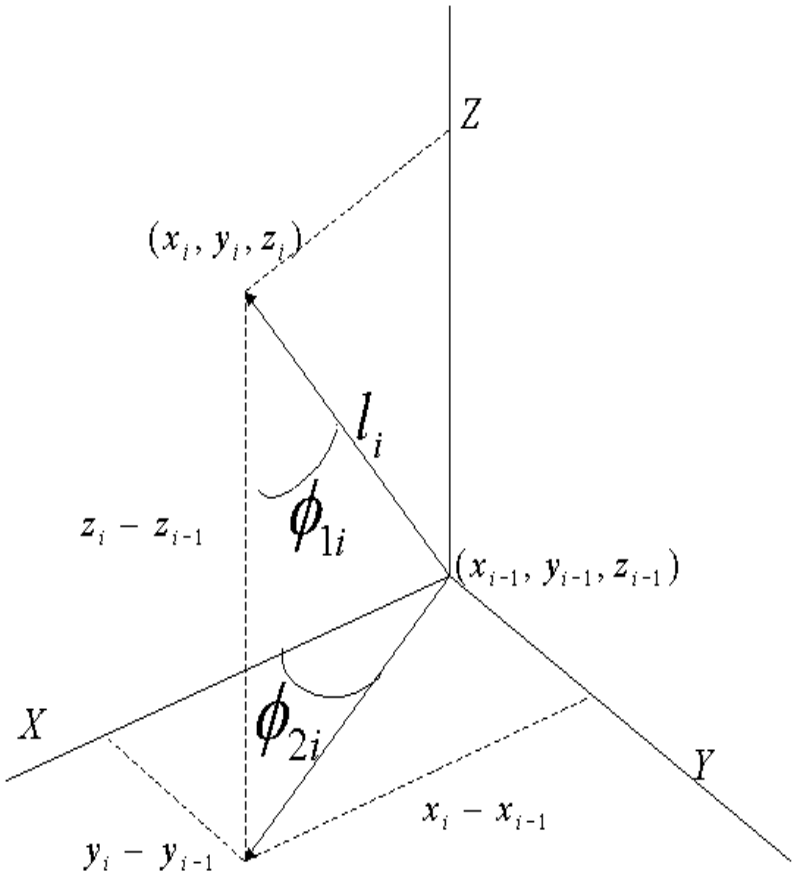


Figure 2:

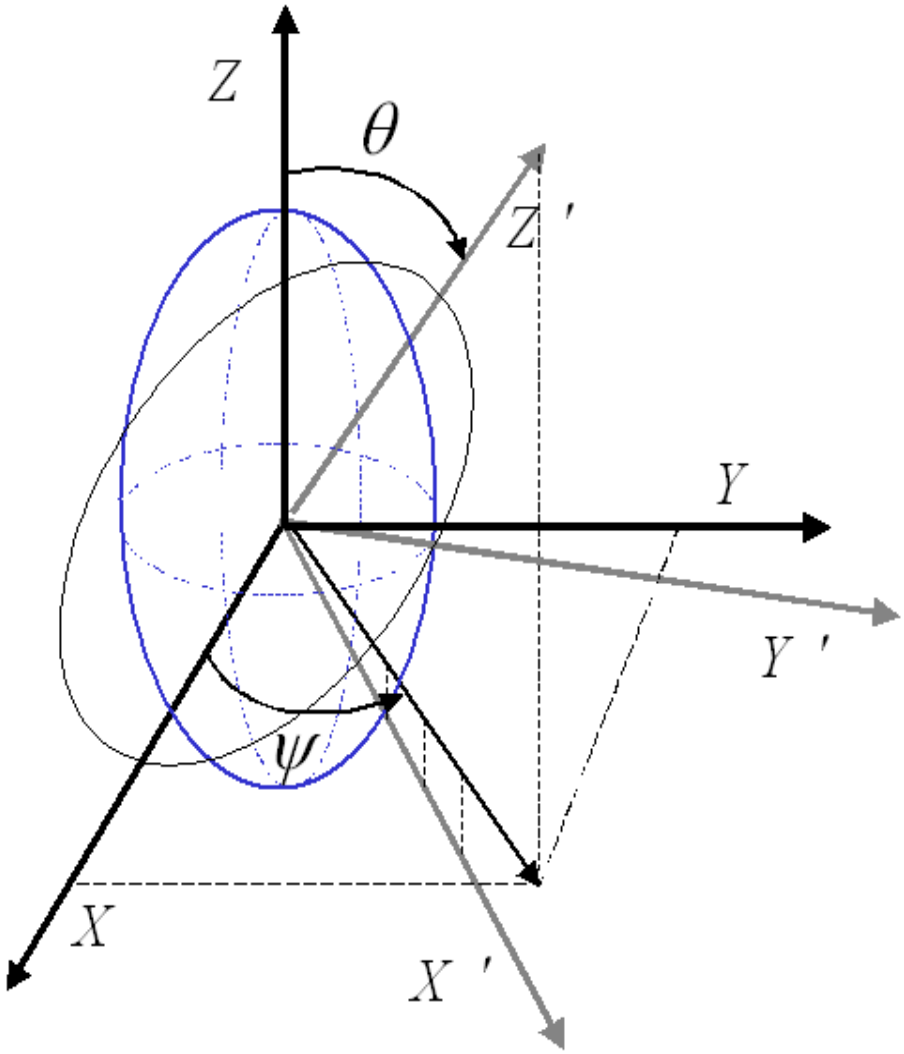


Figure 3:

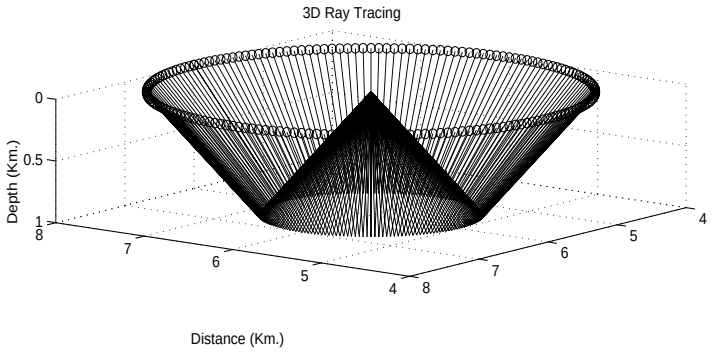


Figure 4:



Figure 5:

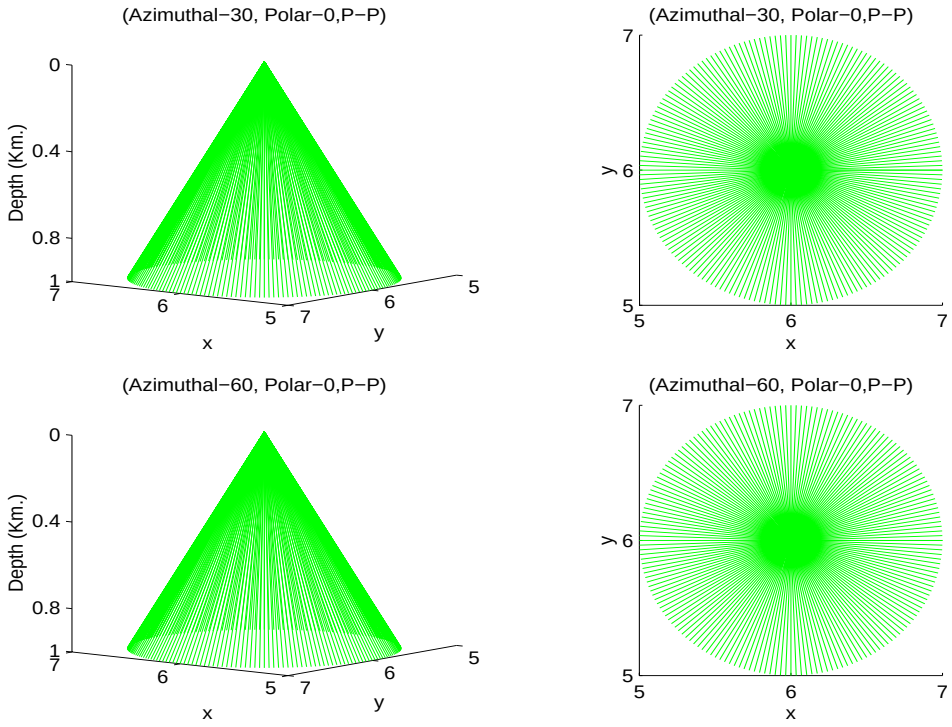

(Azimuthal−30, Polar−0,P−P)
Depth (Km.)
0
0.4
0.8
1
7
6
5
x
7
6
5
y
(Azimuthal−30, Polar−0,P−P)
7
6
5
y
5
6
7
x
(Azimuthal−60, Polar−0,P−P)
Depth (Km.)
0
0.4
0.8
1
7
6
5
x
7
6
5
y
(Azimuthal−60, Polar−0,P−P)
7
6
5
y
5
6
7
x

Figure 6:

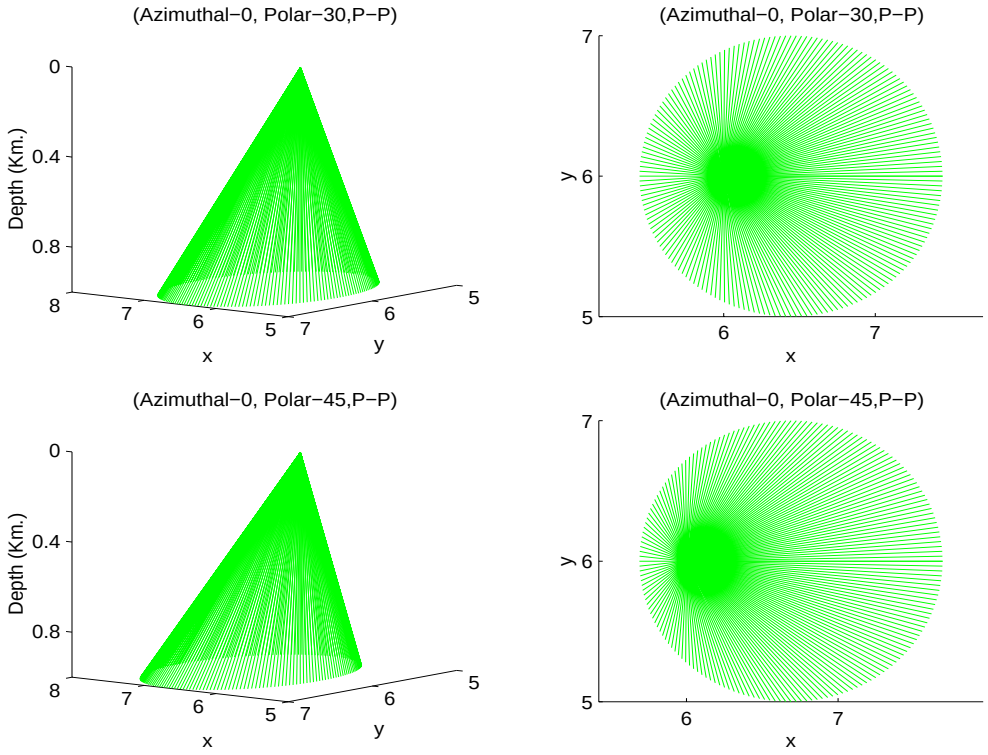

(Azimuthal−0, Polar−30,P−P)
Depth (Km.)
0
0.4
0.8
8
7
6
5
x
7
6
5
y
(Azimuthal−0, Polar−30,P−P)
7
6
5
y
6
7
x
(Azimuthal−0, Polar−45,P−P)
Depth (Km.)
0
0.4
0.8
8
7
6
5
x
7
6
5
y
(Azimuthal−0, Polar−45,P−P)
7
6
5
y
6
7
x

Figure 7:

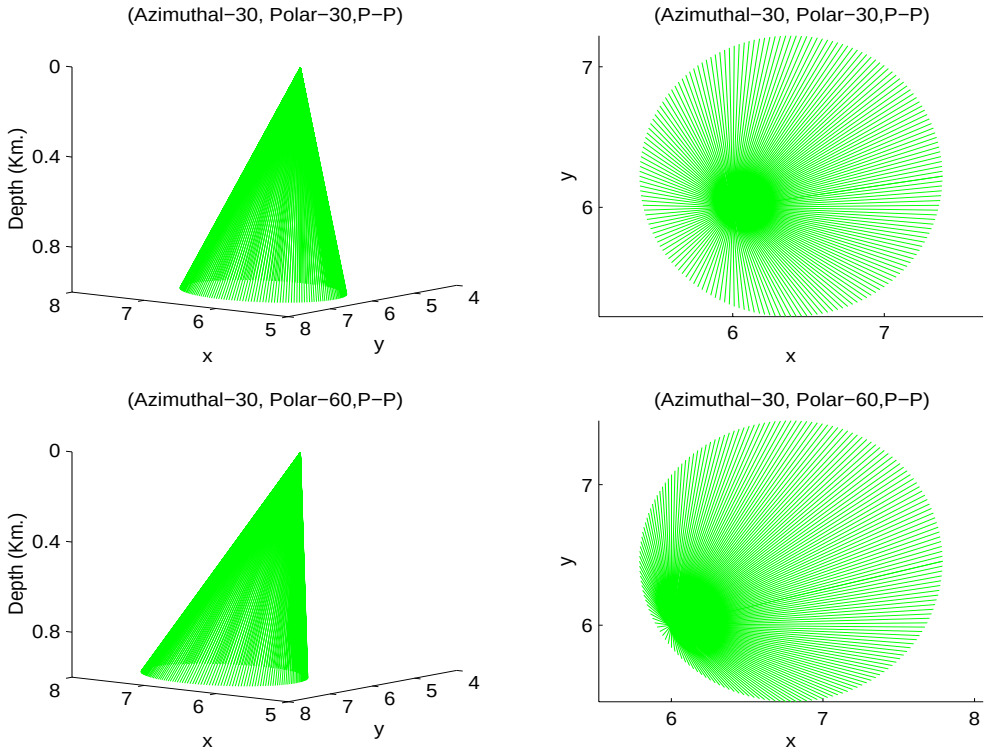

(Azimuthal−30, Polar−30,P−P)
Depth (Km.)
0
0.4
0.8
8
7
6
5
x
8
7
6
5
4
y
(Azimuthal−30, Polar−30,P−P)
7
6
y
6
7
x
(Azimuthal−30, Polar−60,P−P)
Depth (Km.)
0
0.4
0.8
8
7
6
5
x
8
7
6
5
4
y
(Azimuthal−30, Polar−60,P−P)
7
6
y
6
7
8
x

Figure 8:

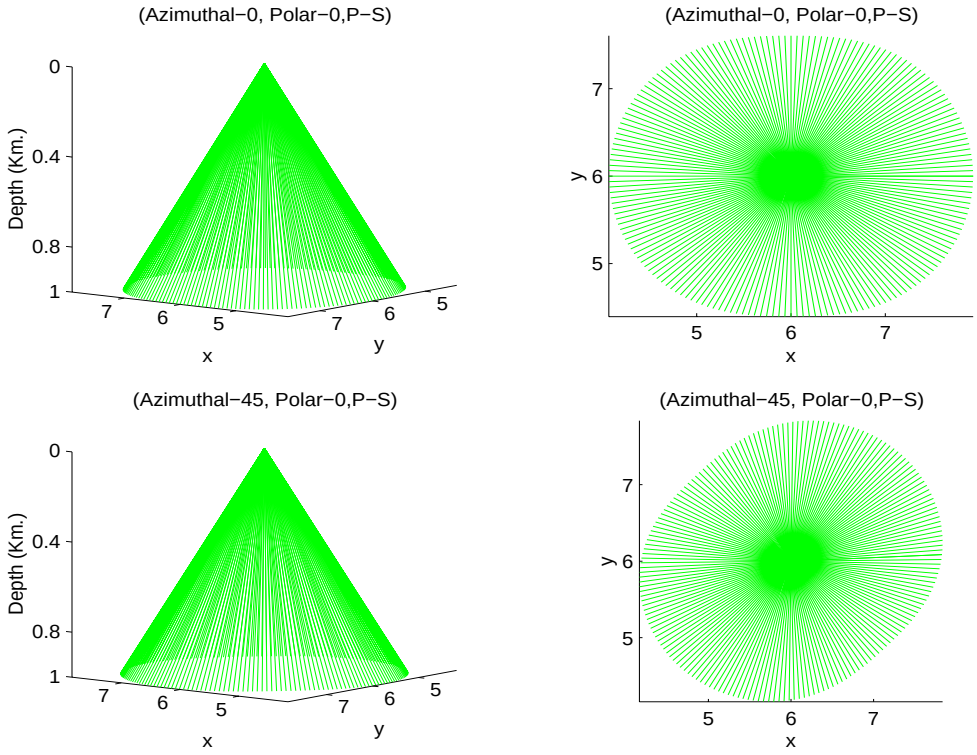

(Azimuthal−0, Polar−0,P−S)
Depth (Km.)
0
0.4
0.8
1
7
6
5
x
7
6
5
y
(Azimuthal−0, Polar−0,P−S)
y
7
6
5
5
6
7
x
(Azimuthal−45, Polar−0,P−S)
Depth (Km.)
0
0.4
0.8
1
7
6
5
x
7
6
5
y
(Azimuthal−45, Polar−0,P−S)
y
7
6
5
5
6
7
x

Figure 9:

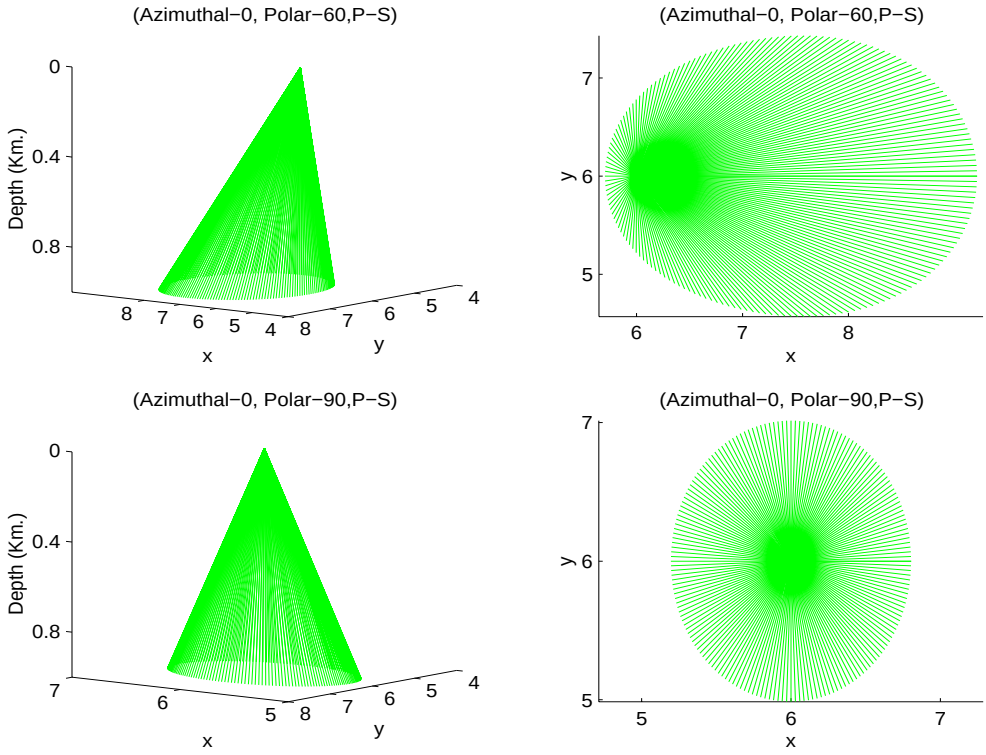

(Azimuthal−0, Polar−60,P−S)
Depth (Km.)
0
0.4
0.8
8 7 6 5 4
x
8 7 6 5 4
y
(Azimuthal−0, Polar−60,P−S)
7
y 6
5
6 7 8
x
(Azimuthal−0, Polar−90,P−S)
Depth (Km.)
0
0.4
0.8
7 6 5
x
8 7 6 5 4
y
(Azimuthal−0, Polar−90,P−S)
7
y 6
5
5 6 7
x

Figure 10:

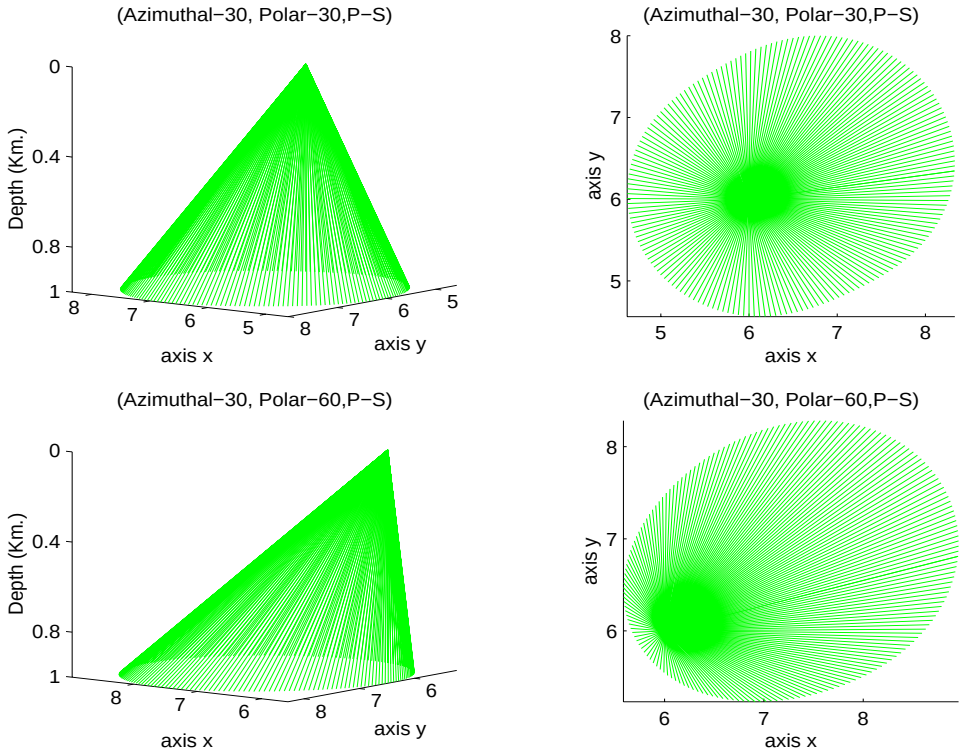

(Azimuthal−30, Polar−30,P−S)
Depth (Km.)
0
0.4
0.8
1
8
7
6
5
8
7
6
5
axis x
axis y
(Azimuthal−30, Polar−30,P−S)
axis y
8
7
6
5
5
6
7
8
axis x
(Azimuthal−30, Polar−60,P−S)
Depth (Km.)
0
0.4
0.8
1
8
7
6
8
7
6
axis x
axis y
(Azimuthal−30, Polar−60,P−S)
axis y
8
7
6
6
7
8
axis x

Figure 11:

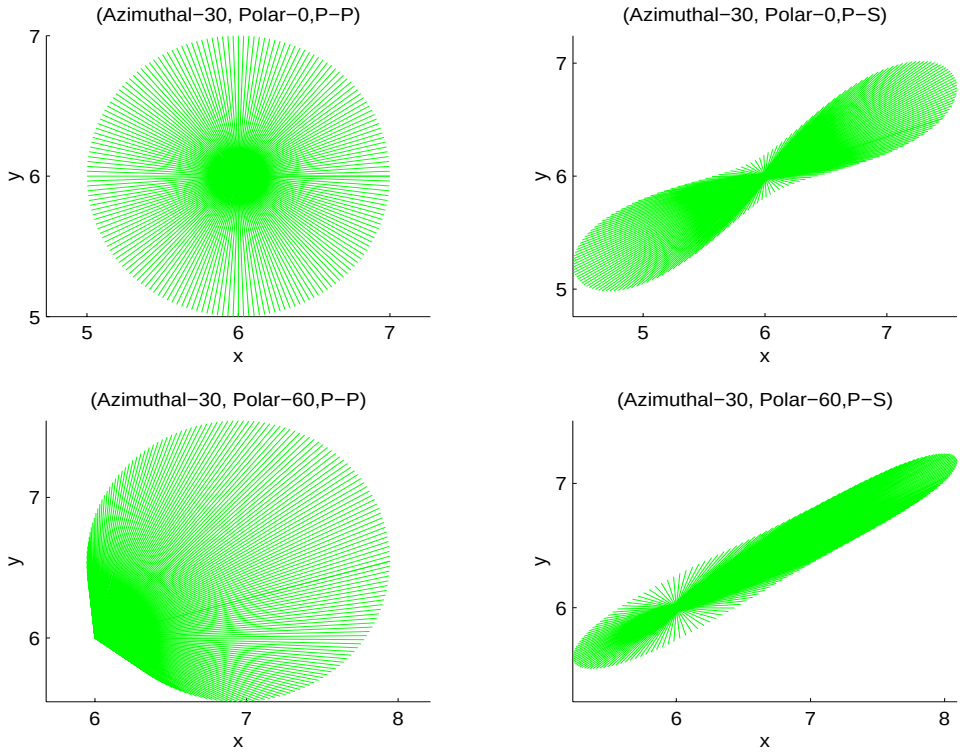

(Azimuthal−30, Polar−0,P−P)
(Azimuthal−30, Polar−0,P−S)
(Azimuthal−30, Polar−60,P−P)
(Azimuthal−30, Polar−60,P−S)
x
y

Figure 12:

		GSG Method		SD Method	
Θ_i	Ψ_i	Total CPU time (sec.)	Δ_{iter}	Total CPU time (sec.)	Δ_{iter}
0	30	8.28	29	376	2762
0	0	8.32	30	378	2778
30	0	10.59	34	531	3797
30	30	10.98	36	548	3920

Table 1:

9 Figure Captions

Figure 1: Parametrization of a general 3D model

Figure 2: Polar and azimuthal group angles

Figure 3: Ellipsoidal orthorhombic medium: polar and azimuthal rotation angles

Figure 4: 3D Ray trajectory for Model 1 in a homogeneous orthorhombic medium

Figure 5: Ray projection for Model 1 in a homogeneous orthorhombic medium

Figure 6: 3D Ray trajectory and its projection for non-converted waves (Test1)

Figure 7: 3D Ray trajectory and its projection for non-converted waves (Test 1)

Figure 8: 3D Ray trajectory and its projection for non-converted waves (Test 1)

Figure 9: 3D Ray trajectory and its projection for converted waves (Test 2)

Figure 10: 3D Ray trajectory and its projection for converted waves (Test 2)

Figure 11: 3D Ray trajectory and its projection for converted waves (Test 2)

Figure 12: 3D Ray trajectory and its projection for converted waves (Test 3)

Table 1: Computational work and CPU time for GSG and SD methods (test4)